Published in final edited form as:
*Mucosal Immunol*. 2018 May ; 11(3): 681–692. doi:10.1038/mi.2017.105.

# CD103$^{+}$CD11b$^{+}$ mucosal classical dendritic cells initiate long-term switched antibody responses to flagellin

**A Flores-Langarica**[1,*], **K Müller Luda**[3], **E K Persson**[3], **C N Cook**[1], **S Bobat**[1], **J L Marshall**[1], **M W Dahlgren**[3], **K Hägerbrand**[3], **K M Toellner**[1], **M D Goodall**[1], **D R Withers**[1], **I R Henderson**[2], **B Johansson Lindbom**[3,4], **A F Cunningham**[1,2,*,#], and **W W Agace**[3,4,#]

[1]Institute of Immunology & Immunotherapy, College of Medical & Dental Sciences, University of Birmingham, Birmingham, B15 2TT, UK

[2]Institute of Microbiology and Infection, College of Medical & Dental Sciences, University of Birmingham, Birmingham, B15 2TT, UK

[3]Immunology Section, Lund University, BMC D14 Sölvegatan 19, S-221 84. Lund 22184, Sweden

[4]Division of Immunology and Vaccinology, National Veterinary Institute, Technical University of Denmark (DTU). Kongens Lyngby, Denmark

## Abstract

Antibody (Ab) responses induced at mucosal and non-mucosal sites demonstrate a significant level of autonomy. Here we demonstrate a key role for mucosal IRF4-dependent CD103$^{+}$CD11b$^{+}$ (DP), classical dendritic cells (cDC) in the induction of T-dependent IgG and IgA responses in the mesenteric lymph node (MLN) following systemic immunization with soluble flagellin (sFliC). In contrast, IRF8-dependent CD103$^{+}$CD11b$^{-}$ (SP) are not required for these responses. The lack of this response correlated with a complete absence of sFliC-specific plasma cells in the MLN, small intestinal lamina propria and surprisingly also the BM. Many sFliC-specific plasma cells accumulating in the BM of immunized wildtype mice expressed $\alpha 4\beta 7^{+}$suggesting a mucosal origin. Collectively these results suggest that mucosal DP cDC, contribute to the generation of the sFliC-specific plasma cell pool in the BM and thus serve as a bridge linking the mucosal and systemic immune system.

## Introduction

Flagellin is the filament protein component of bacterial flagella. Extracellular flagellin is recognised primarily through TLR5 and this can induce profound responses in innate and

[*]Authors for Correspondence: Adriana Flores-Langarica (a.floreslangarica@bham.ac.uk) & Adam F Cunningham (a.f.cunningham@bham.ac.uk). Institute of Immunology & Immunotherapy, College of Medical & Dental Sciences, University of Birmingham, Birmingham, B15 2TT, UK. +44 121 414 6970 (Tel), +44 121 414 3599 (Fax).
[#]Joint senior authors: Adam F Cunningham & William W Agace

**Author contributions**

Conceptualization, AFL, AFC & WA. Methodology, MWD, KH, BNL & BJL. Investigation, AFL, KML, EKP, SB, JM. Resources, CC, DRW. Writing - original draft, AFL, AFC, BJL & WA. Writing - Review & Editing, AFL, AFC, IRH, BJL & WA. Funding Acquisition, AFL, AFC & WA.

**Disclosure**

Authors declare no conflict of interest.


Europe PMC Funders Author Manuscripts

adaptive immune cells1. Immunization with purified, soluble flagellin (sFliC) protein from *Salmonella* Typhimurium (STm) is sufficient to drive T and B cell responses against itself and co-immunized antigens in the absence of additional adjuvant 2–5. This autoadjuvant activity of flagellin has led to it's use as a carrier protein in a number of vaccine strategies6–8, including an influenza fusion vaccine tested in humans9, 10. Additionally, immunization of sFliC in mice has been shown to enhance protection against viral infections 11 and radiation exposure12, promote antigen presentation through MHCII 13 and reduce Th1 differentiation after co-immunization with STm14. While such findings indicate that flagellin is an important modulator of the adaptive immune system, the cellular mechanism(s) underlying it's mode-of-action remain unclear.

Previously, it has been shown that systemic immunization with sFliC, given subcutaneously in the footpad or intraperitoneally, induces IgG responses in the spleen and concurrent IgG and IgA responses in the intestinal draining mesenteric lymph nodes (MLN)15. This unexpected induction of intestinal responses after systemic immunization was TLR5-dependent and associated with the rapid and extensive recruitment of antigen-loaded $CD103^+$ classical dendritic cells (cDC) into the MLN. This coincided with a decrease in the frequency of these cells in the small intestine lamina propria (SI-LP) and suggests that the autoadjuvant activity of sFliC may, in part, be mediated through the activation of mucosal $CD103^+$ cDC.

The intestinal mucosa contains three major subsets of cDC; $CD103^+CD11b^+$, $CD103^+CD11b^-$ and $CD103^-$ cDCs16, 17 that require different transcription factors for their development and survival. Deletion of the transcription factors interferon regulatory factor (IRF) 8, BATF3 or ID2 results in a loss of intestinal and MLN $CD103^+CD11b^-$ cDC18–20 while deletion of IRF4 and NOTCH-2 results in a loss of intestinal derived $CD103^+CD11b^+$ cDC in the MLN 21, 22. We, and others, have recently demonstrated that these subsets play key non-redundant roles in regulating intestinal immune homeostasis. For example, IRF4-dependent cDC play an important role in intestinal Th17 21, 23 and Th2 responses 24 and for driving post-operative ileitis25. In contrast, IRF8 dependent $CD103^+CD11b^-$ cDC are required for the maintenance of T cells within the small intestinal epithelium and for the generation and maintenance of intestinal IFN-γ producing Th1 cells26, 27.

In the current study, we assessed the role of mucosal cDC in the generation of sFliC-specific IgG and IgA responses in MLN following systemic immunization, and the impact of this response on the accumulation of plasma cells in the BM. We demonstrate that mucosal $CD103^+CD11b^+$ but not $CD103^+CD11b^-$ cDC are essential for the generation of sFliC-specific responses in MLN, and that the absence of this response impacts on long-term systemic Ab response in the BM. Collectively these results suggest that mucosal $CD103^+CD11b^+$ cDC act as a bridge to link adaptive immune responses of the intestinal mucosa to serological memory and systemic protection.

## Results

### DP cDCs recruited to the MLN after direct stimulation by sFliC are functional

It has been previously demonstrated that i.p. or s.c. immunization with sFliC drives a TLR5-dependent accumulation of $CD103^+$ cDC in intestinal draining MLN 15. To determine which $CD103^+$ cDC subset in the MLN in response to sFliC, WT mice were immunized i.p. with sFliC and numbers of $CD103^+CD11b^+$ (DP), $CD103^+CD11b^-$ (SP) and $CD103^-$ cDC in the MLN and SI-LP were assessed 24 h later by flow cytometry (for gating strategy see Fig. S1A). sFliC immunized mice had an increased frequency of $CD11c^+MHC\text{-}II^{hi}$ cDC in MLN (Fig. 1A). In the steady-state this population has been shown to contain cDC that have migrated from the SI-LP28 and potentially some resident $CD8\alpha^+$ and $CD11b^+$ cDC that have upregulated MHC-II upon activation. Within the $CD11c^+MHC\text{-}II^{hi}$ population, DP but not SP or $CD103^-$ cDC numbers increased in the MLN in response to sFliC (Fig. 1A), which paralleled a selective loss of DP cDC in the SI-LP (Fig. 1B). Despite the selective increase in DP cDC numbers in MLN, sFliC immunization induced upregulation of CD40 and CD86 in all MLN cDC subsets (Fig. 1C).

sFliC immunization failed to induce DP cDC accumulation in MLN of mice lacking MyD88 in $CD11c^+$ cells (*Cd11c-cre.MyD88*$^{fl/fl}$ mice 28) (Fig. 1D), indicating that sFliC may directly drive DP cDC recruitment to MLN. To assess this possibility, mixed BM chimeras were generated with BM from *Cd11c-cre.Irf4*$^{fl/fl}$ mice, which lack DP cDC in MLN 21 and *Cd11c-cre.MyD88*$^{fl/fl}$ mice (Fig. 1E). In these chimeras, DP cDC in the MLN are MyD88 deficient, while other $CD11c^+$ cells are a mixture of MyD88-sufficient and deficient cells. sFliC also failed to induce DP cDC accumulation in the MLN of these mice (Fig. 1E). *Cd11c-cre.Irf4*$^{fl/fl}$ mice express GFP21 and this can be used as a way to discriminate between cells derived from different donor mice. Assessment of GFP expression in cDCs from the SI-LP of the chimeras showed that both *MyD88*$^{fl/fl}$ ($GFP^-$) and *Cd11c-cre.MyD88*$^{fl/fl}$ cDCs ($GFP^-$) were found in similar proportions in comparison with cDC derived from *Cd11c-cre.Irf4*$^{fl/fl}$ ($GFP^+$) donor BM (Fig. S1B). Collectively these results demonstrate that sFliC signalling in DP cDC is required for their accumulation in the MLN.

It has been previously shown that $CD103^+$ cDC are responsible for T cell priming in the MLN following i.p immunization with sFliC 15. To determine which of the two MLN $CD103^+$ cDC subsets underlie this response SP and DP cDC were FACS sorted from the MLN 24 h after i.p. immunization with sFliC and co-cultured with SM1 transgenic T cells, which are specific for an epitope in *Salmonella* Typhimurium FliC (amino acids 427–441)29, 30. DP cDC were far more efficient than SP cDC at inducing SM1 T cell division and activation as assessed by CFSE dilution, downregulation of CD62L and total cell counts (Fig. 1F). Importantly, *ex vivo* addition of sFliC to the SP and DP cDC-T cell co-cultures resulted in similar SM1 T cell division (Fig. 1F), demonstrating that the diminished capacity of SP cDC to present sFliC *in vivo* was not due to an inability of these cells to present antigen. Thus, DP cDC represent the major sFliC peptide presenting cells in the MLN.

## CD103$^{+}$CD11b$^{+}$ DP cDC are required for the generation of mucosal anti-sFliC IgA and IgG responses

To assess the role of MLN CD103$^{+}$ cDC subsets in sFliC-specific Ab responses, we used a prime-boost system as previously described15. First, we determined whether priming with sFliC, could interfere with the accumulation of DP cDC (for example through the induction of antibodies) after secondary immunization. Secondary immunization induced a similar and selective accumulation of DP cDC in the MLN as observed after primary immunization (Fig. 2A), despite the presence of sFliC-specific IgG in the serum (Fig. 2B).

To address the role of DP cDC in the sFliC-specific Ab response *Cd11c-cre.Irf4$^{fl/fl}$* mice were immunized twice with sFliC and the response was examined 4 d after boost. In marked contrast to control *Irf4$^{fl/fl}$* mice, the number of plasma cells did not increase in the MLN of *Cd11c-cre.Irf4$^{fl/fl}$* mice following boosting with sFliC (Fig. 3A; detailed gating strategy is shown in Fig. S1C), suggesting a reduced sFliC-specific Ab response at this site. Consistent with this, sFliC-specific IgG and IgA Ab-secreting cells (ASC) were readily detected in the MLN of *Irf4$^{fl/fl}$* but not *Cd11c-cre.Irf4$^{fl/fl}$* mice as assessed by ELISPOT (Fig. 3B). Plasma cells derived from the MLN can migrate to the SI-LP contributing to the specific response in this site. To examine whether this element of the response was also affected, cells were isolated from the SI-LP and sFliC-specific ASC assessed as above. As with the MLN, sFliC-specific IgG$^{+}$ and IgA$^{+}$ ASCs were detected in the SI-LP of *Irf4$^{fl/fl}$* but not *Cd11c-cre.Irf4$^{fl/fl}$* mice (Fig. 3B, lower panels). To exclude the possibility that the reduced numbers of sFliC-specific ASC observed in *Cd11c-cre.Irf4$^{fl/fl}$* mice was a result of an intrinsic defect in B cell function 31, mixed bone marrow chimeras were generated using a 50:50 mix of BM cells from *Irf4$^{fl/fl}$* or *Cd11c-cre.Irf4$^{fl/fl}$* mice with BM cells from *Rag-1$^{-/-}$* mice. In these chimeras Irf4-dependent cDC derive from *Rag-1$^{-/-}$* BM while the B cell compartment derives from *Cd11c-cre.Irf4$^{fl/fl}$* BM. RAG-1$^{-/-}$ BM fully rescued the defect in plasma cell numbers observed in single *Cd11c-cre.Irf4$^{fl/fl}$* chimeras (Fig. 3C lower graph) as well as sFliC-specific IgG and IgA producing ASC (Fig. 3C), confirming that the absence of Ab response in the *Cd11c-cre.Irf4$^{fl/fl}$* mice was not due to an intrinsic B cell defect.

In marked contrast to *Cd11c-cre.Irf4$^{fl/fl}$* mice, *Cd11c-cre.Irf8$^{fl/fl}$* mice, which lack migratory SP cDC and LN resident CD8α$^{+}$ cDC in the MLN 26, induced equivalent numbers of plasma cells and anti-sFliC IgG and IgA ASC in the MLN as control *Irf8$^{fl/fl}$* mice, following sFliC prime-boost (Fig. 3D-E). Collectively these results demonstrate that the generation of sFliC-specific Ab responses in the MLN requires DP cDC.

## Tfh cells and GC responses to sFliC in the MLN are absent in *Cd11c-cre.Irf4$^{fl/fl}$* mice

Since the Ab response to sFliC is T-dependent 3, 5 we next assessed whether the absence of a sFliC-specific Ab response in the MLN of *Cd11c-cre.Irf4$^{fl/fl}$* mice reflected alterations in the generation of sFliC-specific GC and Tfh cells. sFliC-specific GCs were readily detected in the MLN of *Irf4$^{fl/fl}$* but not *Cd11c-cre.Irf4$^{fl/fl}$* mice (Fig. 4A) and confocal microscopy showed the presence of PD1 and BCL6 expressing Tfh-like T cells in these GCs (Fig. 4A lower panels). Quantification of the GC and the total sFliC-specific area per section showed that immunized *Irf4$^{fl/fl}$* mice had significantly more area containing GC than immunized *Cd11c-cre.Irf4$^{fl/fl}$* mice (Fig. 4B). Consistent with this finding, GC B cell numbers increased

in sFliC-immunized *Irf4*$^{fl/fl}$ but not *Cd11c-cre.Irf4*$^{fl/fl}$ mice, as determined by flow cytometry (Fig. 4C; for gating strategy see Fig. S1C). Similarly, the total number of Tfh cells (defined as CD3$^+$CD4$^+$CD62L$^{lo}$PD1$^+$CXCR5$^+$, for gating strategy see Fig. S1D) increased in the MLN of *Irf4*$^{fl/fl}$ mice but not in *Cd11c-cre.Irf4*$^{fl/fl}$ mice (Fig. 4D). In contrast, *Cd11c-cre.Irf8*$^{fl/fl}$ mice displayed a similar increase in total GC area, sFliC-specific GC area, GC B cells and Tfh cells in the MLN to *Irf8*$^{fl/fl}$ mice (Fig. 4E-H). Thus, the defective mucosal Ab response observed in the absence of DP cDC is associated with a loss in the generation of Tfh cells and sFliC-specific GCs in MLN.

## sFliC-specific splenic ASCs are reduced in *Cd11c-cre.Irf4*$^{fl/fl}$ mice

As sFliC induces concurrent Ab responses in the spleen and MLN 15 we next determined whether *Cd11c-cre.Irf4*$^{fl/fl}$ mice displayed a defective ASC response in the spleen.

Firstly, we evaluated the cDC response in the spleen after immunization with sFliC. In contrast to the MLN, immunization with sFliC did not affect the frequency or total number of CD4$^+$ or CD8α$^+$ cDCs (Fig. 5A), although it led to increased expression of CD86 and CD40 by both subsets (Fig. 5B). As expected21, splenic CD4$^+$ cDC numbers were reduced in *Cd11c-cre.Irf4*$^{fl/fl}$ compared with *Irf4*$^{fl/fl}$ mice in steady state (Fig. 5A), and this difference was maintained after sFliC immunization.

When assessing the Ab response 4 d after secondary immunisation *Cd11c-cre.Irf4*$^{fl/fl}$ mice displayed a reduction in sFliC-specific IgG$^+$ ASC and virtually no IgA$^+$ ASC when compared with *Irf4*$^{fl/fl}$ mice (Fig. 5C). sFliC-specific GCs were observed in the spleens of *Cd11c-cre.Irf4*$^{fl/fl}$ mice after immunization, albeit to a lesser extent when compared to *Irf4*$^{fl/fl}$ mice (Fig. 5D). Strikingly, splenic GC B cell and Tfh cell numbers were not significantly different in *Irf4*$^{fl/fl}$ and *Cd11c-cre.Irf4*$^{fl/fl}$ mice after sFliC immunization (Fig 5E-F). Thus, in marked contrast to the MLN, IRF4 dependent cDC are not required for Tfh cell generation and GC induction in the spleen in response to sFliC immunization.

We hypothesized that Tfh cells were still detectable in the spleens of *Cd11c-cre.Irf4*$^{fl/fl}$ mice because CD8α$^+$CD11b$^-$ splenic cDC could potentially contribute to antigen presentation. To address this possibility, WT mice were immunized with sFliC for 24 h and CD4$^+$CD11b$^+$ and CD8α$^+$CD11b$^-$ splenic cDC were FACS sorted and co-cultured with SM1 T cells. Both CD4$^+$CD11b$^+$ and CD8α$^+$CD11b$^-$ cDC induced SM1 T cell proliferation although CD8α$^+$CD11b$^-$ cDC did so less efficiently (Fig. 5G). The difference in T cell proliferation after co-culture probably reflects differences in antigen capture *in vivo* rather than an intrinsic difference in their capacity to present antigen as T cell proliferation was similar when sFliC was added to the cultures *ex vivo* (Fig. 5G). Collectively these results suggest that IRF4-dependent and independent cDC contribute to the splenic sFliC-specific response.

## Mucosal DP cDC contribute to sFliC-specific Ab responses in the BM

To study the persistence of the anti-sFliC Ab response, we next examined the BM, representing an important site for maintenance of long-lived PC. Strikingly, while sFliC-specific IgG$^+$ and IgA$^+$ ASC were readily detected in the BM of *Irf4*$^{fl/fl}$ mice they were completely absent in the BM of *Cd11c-cre.Irf4*$^{fl/fl}$ mice (Fig. 6A). In contrast, the BM of *Cd11c-cre.Irf8*$^{fl/fl}$ mice had a similar number of sFliC-specific ASC as control *Irf4*$^{fl/fl}$ mice

(Fig. 6B). The complete lack of sFliC-specific ASC in the BM of *Cd11c-cre.Irf4*$^{fl/fl}$ mice suggested that mucosal DP cDC may contribute to the long-term Ab response in the BM. To assess this possibility, expression of the intestinal-associated signature integrin α4β7 32, 33 was examined on BM sFliC-specific plasma cells from WT mice primed-boosted with sFliC. A sFliC-specific population of plasma cells was detected in the BM of sFliC immunized, but not unimmunized mice, as assessed by flow cytometry (Fig. 6C). Further a proportion of these sFliC-specific, but not non-sFliC-specific BM plasma cells expressed α4β7 (Fig. 6C). Consistent with these findings sFliC-specific cells expressing α4β7 were detected on cytospins preparations of enriched CD138$^{+}$ BM cells from the same mice (Fig. 6D). Finally, the data suggest that loss of DP cDC should have an effect on the total serum antibody response to sFliC. To test this we examined the specific IgG and IgA response to this antigen. IgG titers were >90% reduced in *Cd11c-cre.Irf4*$^{fl/fl}$ mice compared to control mice and IgA was undetectable (Fig. 6E). Collectively, these results suggest that mucosal DP cDC priming of antibody responses in the MLN can enhance sFliC-specific ASC numbers in the BM following i.p immunization with sFliC.

## Discussion

Previously, it has been shown that systemic immunization with sFliC induces parallel Ab responses in systemic and mucosal secondary lymphoid tissues, with the latter responses associated with a rapid TLR5-dependent accumulation of antigen-carrying CD103$^{+}$ cDC in the intestinal-draining MLN 15. Here we demonstrate that mucosal DP cDC are required for the anti-sFliC response in the MLN and provide evidence that plasma cells derived from this response can ultimately take up residence in the BM and contribute to the systemic antibody pool. The ability of sFliC to efficiently engage the mucosal immune system after a systemic immunization may confer a significant advantage to sFLiC containing vaccines, such as the influenza-flagellin fusion vaccine that has shown safety and potential, not only in healthy adults but in the elderly 9, 10, who often induce poor Ab responses 34.

While multiple MLN cDC subsets can induce T cell responses to sFliC after antigen loading *in vitro* 35, we demonstrate here that only DP cDC drive T and B cell responses in the MLN *in vivo*. The reasons why IRF4 dependent DP cDC are so critical in driving sFliC-specific T cell responses in the MLN remain to be fully elucidated but are likely multi-factorial. Previous studies have demonstrated that IRF4 dependent cDC have an enhanced intrinsic capacity to prime CD4$^{+}$ T cells compared with IRF8 dependent cDC 23, 36. Interestingly, sFliC induced MyD88-dependent accumulation was similar after secondary immunization, even in the presence of high-affinity sFliC Ab 2, 3, indicating a high efficiency of sFliC capture by TLR5. These results are consistent with prior observations that small amounts of sFliC are required for its immune modulatory effects 37 and further suggest that inclusion of sFliC in boost as well as in prime vaccines could further promote mucosal immune system engagement. Notably, recognition of intestinal microbiota derived flagellin is also TLR5 dependent and boosts vaccine responses through the action of clodronate-sensitive (presumably monocyte derived) cells38. Given our current findings, the cross-talk between these cells and DP cDC in driving the microbiota-derived flagellin response warrants further study. sFliC-specific responses in the spleen were reduced in *Cd11c-cre.Irf4*$^{fl/fl}$ mice. Splenic CD4$^{+}$ cDC from immunized WT mice efficiently primed sFliC-specific T cells *ex*

*vivo* and these cells were selective reduced in *Cd11c-cre.Irf4*$^{fl/fl}$ mice collectively indicating that IRF4-dependent CD4$^{+}$ cDC are required for optimal sFliC-specific responses in the spleen. Despite these findings, sFliC-induced Tfh cell accumulation was not significantly altered, and sFliC-specific GC were readily detectable in the spleen in the absence of IRF4 dependent cDC, suggesting that additional APC contribute to the sFliC-specific response at this site. While the identity of these IRF4-independent APC remains to be identified, splenic CD8$^{+}$ cDC isolated from immunized mice induced limited sFliC-specific T cell generation *ex vivo*, indicating that IRF8-dependent cDC may contribute to this response. Collectively, these findings indicate that the cellular and molecular mechanism driving sFliC-specific immune responses in the spleen and MLN are, in part, distinct.

These findings are consistent with prior studies demonstrating that immune responses induced by sFliC are both complex and site-specific. Thus, while sFliC drives both an IgG and IgA response in the MLN, it drives primarily an IgG response in the spleen 15. sFliC-specific IgA responses are TLR5-dependent 15, whereas sFliC-specific IgG responses, in particular IgG1 responses, can occur through TLR5- and inflammasome-independent pathways 13, 39. Furthermore sFliC-specific T cell responses in the spleen are also less dependent on TLR5 than in the MLN 15 and splenic cDCs have been reported to express lower levels of TLR5 in comparison to cDC from the intestinal mucosa 40. Thus the features of sFliC that enable it to have these effects are likely to relate to it being the ligand for TLR5 and its modest molecular size. The accumulation of CD103$^{+}$ cDCs in the MLN after sFliC immunization is TLR5 dependent41 and SI-LP cDCs with a similar phenotype as DP cDC (CD103$^{+}$CD11c$^{hi}$CD11b$^{hi}$) have been shown to express high levels of TLR5 42. In contrast, splenic cDCs do not appear to express as high levels of TLR5 as SI-LP cDCs40. Indeed, consistent with the need for TLR5 expression, we show that MyD88 expression in DP cDCs is needed for their accumulation in the MLN after immunization. Furthermore, TLR5 itself can enhance presentation of antigen through MyD88-independent mechanisms, indicating its function in promoting antigen presentation may be multifactorial13. Although these points may help explain why DP cDCs have an enhanced capacity to capture and present sFliC, it does not explain how sFliC gets to this site. This could relate to the use of highly purified, monomeric flagellin in these studies. This soluble protein has a relatively modest size of ~50kDa, meaning it can disseminate readily through the host after systemic immunization. Other studies have found molecules of a similar or greater size are also able to disperse rapidly throughout the host and prime responses in multiple sites43. Another potential mechanism through which DP cDCs may drive these responses to sFliC is through their potential interactions with B cells. This possibility was not addressed in the current study, but is worthy of future study. Therefore, a more detailed understanding of the molecular pathways by which APC subsets orchestrate these diverse responses to sFliC should provide important information regarding sFliC usage in future vaccines.

Interestingly, IgA$^{+}$ and IgG$^{+}$ sFliC-specific ASC were completely absent in the BM of sFliC immunized *Cd11c-cre.Irf4*$^{fl/fl}$ mice and we found that a proportion of sFliC-specific ASC accumulating in the BM of sFliC immunized WT mice expressed the intestinal homing receptor α4β7. This suggests that some of these ASC were initially generated in intestinal lymph nodes 44. Nevertheless, this does not necessarily mean all ASC in the BM derive from the mucosa, nor does it exclude the possibility that long-lived ASC can be generated in

other sites, since we detected sFliC-specific ASC in the spleen. For instance, it has been shown that long-lived plasma cells can be found in the spleen, as well as the BM, indicating multiple reservoirs can exist45. Collectively these results suggest that the priming of responses in the MLN by DP cDC may contribute to the accumulation of sFliC-specific plasma cells in the BM and hence to sFliC-specific serological memory. In support of this, sFliC-specific $IgA^+$ PC are detected in the MLN and not the spleen during a primary response 15 and long-lived BM plasma cell responses can be induced in splenectomised mice after immunizing mice orally with high doses of ovalbumin and cholera toxin 46. The ability of sFliC to engage DP cDCs, and in so doing promote both mucosal and serological antibody responses, could mean that optimal serological memory requires engagement of the mucosa. Alternatively, this effect could be restricted to the response to sFliC, or just last for the period assessed in this study. Indeed, the ablated ASC response in the MLN and SI-LP observed when mucosal DP cDCs were reduced was not observed in the spleen, indicating that other pathways for the generation of ASCs remain. Thus, this reduction in ASC in the BM may not be permanent or absolute. Either way, it suggests it may be possible to use flagellin to direct mucosally-induced plasma cells to the BM. Understanding this may help identify how to enhance the longevity of responses to vaccines, which can be dramatically different depending upon their nature and how they are administered47.

In summary, our results show how sFliC, by targeting DP cDC, can overcome the difficulties in inducing a mucosal response after systemic immunization. This highlights the interplay between the mucosal and systemic immune systems and offers an alternative and highly desirable approach to drive long-lived systemic immunity by engaging mucosal DP cDC.

## Methods

### Mice

*Cd11c-cre.MyD88*$^{fl/fl}$ *28, Cd11c-cre.Irf4*$^{fl/f}$ 21 and *Cd11c-creIrf8*$^{fl/fl}$ mice26 were maintained at the Biomedical Center, at Lund University. SM1 transgenic 29 mice were maintained at the University of Birmingham Biomedical Service Unit. Specific pathogen-free 6–8 wk C57BL/6 mice were purchased from Harlan Sprague-Dawley. Littermates or age matched mice were used for all experiments where appropriate. All animal procedures were carried out in strict accordance with the Lund/Malmö Animal Ethics Committee, the University of Birmingham Ethics Committee and UK Home Office approval (project license 30/2850).

### Antigen preparation and immunizations

sFliC was generated as described 3. Briefly, the FliC gene from STm was cloned into $pETT22b^+$ via *ndeI* and *xhoI* sites to incorporate a poly-histidine tag. After induction, His-tagged recombinant protein was enriched by nickel affinity chromatography resulting in a purity of 95%. Following dialysis, the protein was further purified by immunoprecipitation with a sFliC-specific monoclonal. Each batch was tested by immunization of WT and TLR5-deficient mice. Batches were only accepted if cDC in the spleen and MLN matured in WT but not TLR5-deficient mice. Mice were immunized i.p. with 20 μg recombinant sFliC, i.p boosted 21 d later with the same dose and responses were assessed 4 d post-boost.

### Cell isolation and flow cytometry

Single cell suspensions from spleen and MLN and BM were generated by mechanical disruption. When evaluating cDC, MLN and spleen were enzymatic digested with collagenase IV digestion (400 U/ml; 25 min; 37°C). Cell suspensions from SI-LP were generated as previously described 48 using Liberase TM (0.2-0.3 WunchU/ml, Roche). Cells were processed for flow cytometry according to standard procedures 15. Data acquisition was performed on a LSRII (BD Bioscience) or a CyAn ADP (Beckman Coulter) and analysed using FlowJo software 9.8.2. (Tree Star). All antibodies used are listed in Table S1.

### Mixed BM chimeras

BM chimeras were generated by transferring BM cells ($1.5x10^6$ cells) i.v. from the indicated donor mice into lethally irradiated (900 rad) recipient mice. Mixed BM chimeras were generated by transferring a 50:50 mix of BM from the indicated strains. Mice were used for immunization experiments 8 w after BM transfer.

### In vitro co-culture to evaluate cDC antigen loading in vivo

Spleen and MLN were collected 24 h post i.p immunization with sFliC (20 μg), and single-cell suspensions prepared as described above. cDC were pre-enriched using MACS beads (anti-CD19, CD5 and DX5). Cell suspensions were subsequently stained with anti-CD11c, MHC-II, CD103 and CD11b (MLN) or CD11c, MHCII, CD4 and CD8 (spleen) and the indicated cDC subsets FACS sorted on a BD FACSAria Fusion. The following subsets were isolated: SP ($CD103^+CD11b^-$) and DP ($CD103^+CD11b^+$) cDC from the MLN from the $CD11c^{hi}MHC\text{-}II^+$ population. From the spleen using again a pregate $CD11c^{hi}MHC\text{-}II^+$ $CD8\alpha^+CD11b^-$ and $CD4^+CD11b^+$ cDC were sorted to a purity of at least 97%. SM1 T cells were MACS enriched ($CD5^+$ selection) and CFSE labelled. cDC and T cells were co-cultured for 4 d (1:30 ratio cDC/T) before flow cytometry analysis.

### ELISPOT analysis

ELISPOT was performed as described previously 15. In brief, $5x10^5$ cells were added per well in triplicates, in a sFliC pre-coated plate and cultured for 6 h at 37°C. After incubation, plates were incubated overnight at 4°C with alkaline phosphate conjugated anti-IgG and IgA (Southern Biotech). Reaction was developed with SIGMA Fast BCIP®/NBT (Sigma Aldrich). Spots were counted using the AID ELISPOT Reader System and AID software version 3.5 (Autoimmune Diagnostika). Counts were expressed as SFUs/$5x10^5$ cells.

### Immunohistochemistry and confocal microscopy

Immunohistology was performed as described previously 3. Cryosections were incubated with primary unconjugated Abs for 45 min at RT before addition of either HRP-conjugated or biotin-conjugated secondary antibodies. sFliC-binding cells were identified as described 3, 15 using biotinylated sFliC. When using cytospins, $1x10^5$ cells were used per cytospin and cells were fixed in cold acetone for 10 min. Signal was detected using diaminobenzidine for HRP activity and naphthol AS-MX phosphate with Fast Blue salt and levamisole for alkaline phosphatase activity. Images were acquired using a Leica microscope DM6000

using 10x and 20x objectives or the Zeiss Axio ScanZ1 Slide Scanner using 10x objective. Quantification of GC area was performed using Zen 2012 (blue edition) software.

Confocal was performed on frozen sections as previously described 49. Staining was performed in PBS containing 10% FCS, 0.1% sodium azide and sections were mounted in 2.5% 1,4-Diazabicyclo(2,2,2)octane (pH 8.6) in 90% glycerol in PBS. Confocal images were acquired using a Zeiss LSM510 laser scanning confocal microscope with a Zeiss AxioVert 100M. Signals obtained from lasers were scanned separately and stored in four non-overlapping channels as pixel digital arrays of 2048x2048 (10X objective) or 1024x1024 (63X objective).

### FliC-specific ELISA

ELISA plates were coated with 5 μg/ml of sFliC (2 h at 4°C) and blocked with 1% BSA overnight at 4°C. Serum, diluted 1:100 in PBS-0.05% Tween, was added and diluted stepwise. To measure total Ab titres serum was diluted in 1:1000 and added and further diluted stepwise on uncoated plates. Following incubation for 1 h at 37°C, plate-bound antibodies were detected using alkaline phosphatase conjugated goat anti-mouse IgG, IgG1, and IgA (Southern Biotech). Reaction was developed with Sigma-Fast p-nitrophenylphosphate (Sigma Aldrich). Relative reciprocal titres were calculated by measuring the dilution at which the serum reached a defined $OD^{405}$.

### Statistics

Statistics were calculated using the nonparametric Mann-Whitney sum of ranks test or two way ANOVA as appropriate using the GraphPad Prism software (GraphPad).

## Supplementary Material

Refer to Web version on PubMed Central for supplementary material.

## Acknowledgments

This work was supported by grants from the BBSRC UK to AFC, U21 staff fellowship program and Wellcome Trust ISSF Mobility grant to AFL, and grants from the Danish Council for Independent Research (Sapere Aude III) and the Swedish Medical Research Council to WA. The authors would like to thank Dr B. N. Lambrecht for original provision of *Irf8*$^{fl/fl}$ mice. We are grateful to Dr K. Kotarsky and A. Selberg for animal typing and husbandry (Lund University), Matthew Graeme MacKenzie for cell sorting and Ian Ricketts at the Biomedical Service Unit at the University of Birmingham.

## References

1. Hayashi F, Smith KD, Ozinsky A, Hawn TR, Yi EC, Goodlett DR, et al. The innate immune response to bacterial flagellin is mediated by Toll-like receptor 5. Nature. 2001; 410(6832):1099–1103. [PubMed: 11323673]
2. Bobat S, Flores-Langarica A, Hitchcock J, Marshall JL, Kingsley RA, Goodall M, et al. Soluble flagellin, FliC, induces an Ag-specific Th2 response, yet promotes T-bet-regulated Th1 clearance of Salmonella typhimurium infection. European journal of immunology. 2011; 41(6):1606–1618. [PubMed: 21469112]
3. Cunningham AF, Khan M, Ball J, Toellner KM, Serre K, Mohr E, et al. Responses to the soluble flagellar protein FliC are Th2, while those to FliC on Salmonella are Th1. Eur J Immunol. 2004; 34(11):2986–2995. [PubMed: 15384042]

Europe PMC Funders Author Manuscripts


4. Didierlaurent A, Ferrero I, Otten LA, Dubois B, Reinhardt M, Carlsen H, et al. Flagellin promotes myeloid differentiation factor 88-dependent development of Th2-type response. J Immunol. 2004; 172(11):6922–6930. [PubMed: 15153511]
5. McSorley SJ, Ehst BD, Yu Y, Gewirtz AT. Bacterial flagellin is an effective adjuvant for CD4+ T cells in vivo. J Immunol. 2002; 169(7):3914–3919. [PubMed: 12244190]
6. Kajikawa A, Zhang L, Long J, Nordone S, Stoeker L, LaVoy A, et al. Construction and immunological evaluation of dual cell surface display of HIV-1 gag and Salmonella enterica serovar Typhimurium FliC in Lactobacillus acidophilus for vaccine delivery. Clin Vaccine Immunol. 2012; 19(9):1374–1381. [PubMed: 22761297]
7. Liu G, Tarbet B, Song L, Reiserova L, Weaver B, Chen Y, et al. Immunogenicity and efficacy of flagellin-fused vaccine candidates targeting 2009 pandemic H1N1 influenza in mice. PLoS One. 2011; 6(6):e20928. [PubMed: 21687743]
8. Sun Y, Shi W, Yang JY, Zhou DH, Chen YQ, Zhang Y, et al. Flagellin-PAc fusion protein is a high-efficacy anti-caries mucosal vaccine. J Dent Res. 2012; 91(10):941–947. [PubMed: 22895510]
9. Taylor DN, Treanor JJ, Strout C, Johnson C, Fitzgerald T, Kavita U, et al. Induction of a potent immune response in the elderly using the TLR-5 agonist, flagellin, with a recombinant hemagglutinin influenza-flagellin fusion vaccine (VAX125, STF2.HA1 SI). Vaccine. 2011; 29(31): 4897–4902. [PubMed: 21596084]
10. Turley CB, Rupp RE, Johnson C, Taylor DN, Wolfson J, Tussey L, et al. Safety and immunogenicity of a recombinant M2e-flagellin influenza vaccine (STF2.4xM2e) in healthy adults. Vaccine. 2011; 29(32):5145–5152. [PubMed: 21624416]
11. Zhang B, Chassaing B, Shi Z, Uchiyama R, Zhang Z, Denning TL, et al. Viral infection. Prevention and cure of rotavirus infection via TLR5/NLRC4-mediated production of IL-22 and IL-18. Science. 2014; 346(6211):861–865. [PubMed: 25395539]
12. Burdelya LG, Krivokrysenko VI, Tallant TC, Strom E, Gleiberman AS, Gupta D, et al. An agonist of toll-like receptor 5 has radioprotective activity in mouse and primate models. Science. 2008; 320(5873):226–230. [PubMed: 18403709]
13. Letran SE, Lee SJ, Atif SM, Uematsu S, Akira S, McSorley SJ. TLR5 functions as an endocytic receptor to enhance flagellin-specific adaptive immunity. Eur J Immunol. 2011; 41(1):29–38. [PubMed: 21182074]
14. Flores-Langarica A, Bobat S, Marshall JL, Yam-Puc JC, Cook CN, Serre K, et al. Soluble flagellin coimmunization attenuates Th1 priming to Salmonella and clearance by modulating dendritic cell activation and cytokine production. Eur J Immunol. 2015; 45(8):2299–2311. [PubMed: 26036767]
15. Flores-Langarica A, Marshall JL, Hitchcock J, Cook C, Jobanputra J, Bobat S, et al. Systemic flagellin immunization stimulates mucosal CD103+ dendritic cells and drives Foxp3+ regulatory T cell and IgA responses in the mesenteric lymph node. Journal of immunology. 2012; 189(12): 5745–5754.
16. Bekiaris V, Persson EK, Agace WW. Intestinal dendritic cells in the regulation of mucosal immunity. Immunol Rev. 2014; 260(1):86–101. [PubMed: 24942684]
17. Joeris T, Muller-Luda K, Agace WW, Mowat AM. Diversity and functions of intestinal mononuclear phagocytes. Mucosal Immunol. 2017
18. Edelson BT, Kc W, Juang R, Kohyama M, Benoit LA, Klekotka PA, et al. Peripheral CD103+ dendritic cells form a unified subset developmentally related to CD8alpha+ conventional dendritic cells. J Exp Med. 2010; 207(4):823–836. [PubMed: 20351058]
19. Ginhoux F, Liu K, Helft J, Bogunovic M, Greter M, Hashimoto D, et al. The origin and development of nonlymphoid tissue CD103+ DCs. J Exp Med. 2009; 206(13):3115–3130. [PubMed: 20008528]
20. Welty NE, Staley C, Ghilardi N, Sadowsky MJ, Igyarto BZ, Kaplan DH. Intestinal lamina propria dendritic cells maintain T cell homeostasis but do not affect commensalism. J Exp Med. 2013; 210(10):2011–2024. [PubMed: 24019552]
21. Persson EK, Uronen-Hansson H, Semmrich M, Rivollier A, Hagerbrand K, Marsal J, et al. IRF4 transcription-factor-dependent CD103(+)CD11b(+) dendritic cells drive mucosal T helper 17 cell differentiation. Immunity. 2013; 38(5):958–969. [PubMed: 23664832]

Europe PMC Funders Author Manuscripts


22. Satpathy AT, Briseno CG, Lee JS, Ng D, Manieri NA, Kc W, et al. Notch2-dependent classical dendritic cells orchestrate intestinal immunity to attaching-and-effacing bacterial pathogens. Nat Immunol. 2013; 14(9):937–948. [PubMed: 23913046]
23. Schlitzer A, McGovern N, Teo P, Zelante T, Atarashi K, Low D, et al. IRF4 transcription factor-dependent CD11b+ dendritic cells in human and mouse control mucosal IL-17 cytokine responses. Immunity. 2013; 38(5):970–983. [PubMed: 23706669]
24. Mayer JU, Demiri M, Agace WW, MacDonald A, Svensson-Frej M, Milling SW. Distinct subsets of IRF4+ dendritic cells drive Th2 responses in the small intestine and colon. Nature Communications. 2017 In Press.
25. Gutweiler S, Pohl J-M, Thiebes S, Gunzer M, Jung S, Agace WW, Kurts C, Engel DR. IRF4-dependent CD103+CD11b+ DCs and microbial signals critically regulate peristalsis and its cessation after intestinal surgery. Gut. 2017 In Press.
26. Luda KM, Joeris T, Persson EK, Rivollier A, Demiri M, Sitnik KM, et al. IRF8 Transcription-Factor-Dependent Classical Dendritic Cells Are Essential for Intestinal T Cell Homeostasis. Immunity. 2016; 44(4):860–874. [PubMed: 27067057]
27. Ohta T, Sugiyama M, Hemmi H, Yamazaki C, Okura S, Sasaki I, et al. Crucial roles of XCR1-expressing dendritic cells and the XCR1-XCL1 chemokine axis in intestinal immune homeostasis. Sci Rep. 2016; 6:23505. [PubMed: 27005831]
28. Hagerbrand K, Westlund J, Yrlid U, Agace W, Johansson-Lindbom B. MyD88 Signaling Regulates Steady-State Migration of Intestinal CD103+ Dendritic Cells Independently of TNF-alpha and the Gut Microbiota. J Immunol. 2015
29. McSorley SJ, Asch S, Costalonga M, Reinhardt RL, Jenkins MK. Tracking salmonella-specific CD4 T cells in vivo reveals a local mucosal response to a disseminated infection. Immunity. 2002; 16(3):365–377. [PubMed: 11911822]
30. McSorley SJ, Cookson BT, Jenkins MK. Characterization of CD4+ T cell responses during natural infection with Salmonella typhimurium. J Immunol. 2000; 164(2):986–993. [PubMed: 10623848]
31. Willis SN, Good-Jacobson KL, Curtis J, Light A, Tellier J, Shi W, et al. Transcription factor IRF4 regulates germinal center cell formation through a B cell-intrinsic mechanism. J Immunol. 2014; 192(7):3200–3206. [PubMed: 24591370]
32. Mei HE, Yoshida T, Sime W, Hiepe F, Thiele K, Manz RA, et al. Blood-borne human plasma cells in steady state are derived from mucosal immune responses. Blood. 2009; 113(11):2461–2469. [PubMed: 18987362]
33. Rott LS, Briskin MJ, Butcher EC. Expression of alpha4beta7 and E-selectin ligand by circulating memory B cells: implications for targeted trafficking to mucosal and systemic sites. J Leukoc Biol. 2000; 68(6):807–814. [PubMed: 11129647]
34. Pinti M, Appay V, Campisi J, Frasca D, Fulop T, Sauce D, et al. Aging of the immune system: Focus on inflammation and vaccination. Eur J Immunol. 2016; 46(10):2286–2301. [PubMed: 27595500]
35. Atif SM, Uematsu S, Akira S, McSorley SJ. CD103-CD11b+ dendritic cells regulate the sensitivity of CD4 T-cell responses to bacterial flagellin. Mucosal Immunol. 2014; 7(1):68–77. [PubMed: 23632327]
36. Vander Lugt B, Khan AA, Hackney JA, Agrawal S, Lesch J, Zhou M, et al. Transcriptional programming of dendritic cells for enhanced MHC class II antigen presentation. Nat Immunol. 2014; 15(2):161–167. [PubMed: 24362890]
37. Lu Y, Swartz JR. Functional properties of flagellin as a stimulator of innate immunity. Sci Rep. 2016; 6:18379. [PubMed: 26755208]
38. Oh JZ, Ravindran R, Chassaing B, Carvalho FA, Maddur MS, Bower M, et al. TLR5-mediated sensing of gut microbiota is necessary for antibody responses to seasonal influenza vaccination. Immunity. 2014; 41(3):478–492. [PubMed: 25220212]
39. Lopez-Yglesias AH, Zhao X, Quarles EK, Lai MA, VandenBos T, Strong RK, et al. Flagellin induces antibody responses through a TLR5- and inflammasome-independent pathway. J Immunol. 2014; 192(4):1587–1596. [PubMed: 24442437]
40. Feng T, Cong Y, Alexander K, Elson CO. Regulation of Toll-like receptor 5 gene expression and function on mucosal dendritic cells. PLoS One. 2012; 7(4):e35918. [PubMed: 22545147]

41. Flores-Langarica A, Marshall JL, Hitchcock J, Cook C, Jobanputra J, Bobat S, et al. Systemic flagellin immunization stimulates mucosal CD103+ dendritic cells and drives Foxp3+ regulatory T cell and IgA responses in the mesenteric lymph node. J Immunol. 2012; 189(12):5745–5754. [PubMed: 23152564]
42. Fujimoto K, Karuppuchamy T, Takemura N, Shimohigoshi M, Machida T, Haseda Y, et al. A new subset of CD103+CD8alpha+ dendritic cells in the small intestine expresses TLR3, TLR7, and TLR9 and induces Th1 response and CTL activity. Journal of immunology. 2011; 186(11):6287–6295.
43. Bonifaz LC, Bonnyay DP, Charalambous A, Darguste DI, Fujii S, Soares H, et al. In vivo targeting of antigens to maturing dendritic cells via the DEC-205 receptor improves T cell vaccination. J Exp Med. 2004; 199(6):815–824. [PubMed: 15024047]
44. Mora JR, von Andrian UH. Differentiation and homing of IgA-secreting cells. Mucosal Immunol. 2008; 1(2):96–109. [PubMed: 19079167]
45. Sze DM, Toellner KM, Garcia de Vinuesa C, Taylor DR, MacLennan IC. Intrinsic constraint on plasmablast growth and extrinsic limits of plasma cell survival. J Exp Med. 2000; 192(6):813–821. [PubMed: 10993912]
46. Lemke A, Kraft M, Roth K, Riedel R, Lammerding D, Hauser AE. Long-lived plasma cells are generated in mucosal immune responses and contribute to the bone marrow plasma cell pool in mice. Mucosal immunology. 2016; 9(1):83–97. [PubMed: 25943272]
47. Slifka MK, Antia R, Whitmire JK, Ahmed R. Humoral immunity due to long-lived plasma cells. Immunity. 1998; 8(3):363–372. [PubMed: 9529153]
48. Jaensson E, Uronen-Hansson H, Pabst O, Eksteen B, Tian J, Coombes JL, et al. Small intestinal CD103+ dendritic cells display unique functional properties that are conserved between mice and humans. J Exp Med. 2008; 205(9):2139–2149. [PubMed: 18710932]
49. Mohr E, Serre K, Manz RA, Cunningham AF, Khan M, Hardie DL, et al. Dendritic cells and monocyte/macrophages that create the IL-6/APRIL-rich lymph node microenvironments where plasmablasts mature. J Immunol. 2009; 182(4):2113–2123. [PubMed: 19201864]

Europe PMC Funders Author Manuscripts

Europe PMC Funders Author Manuscripts

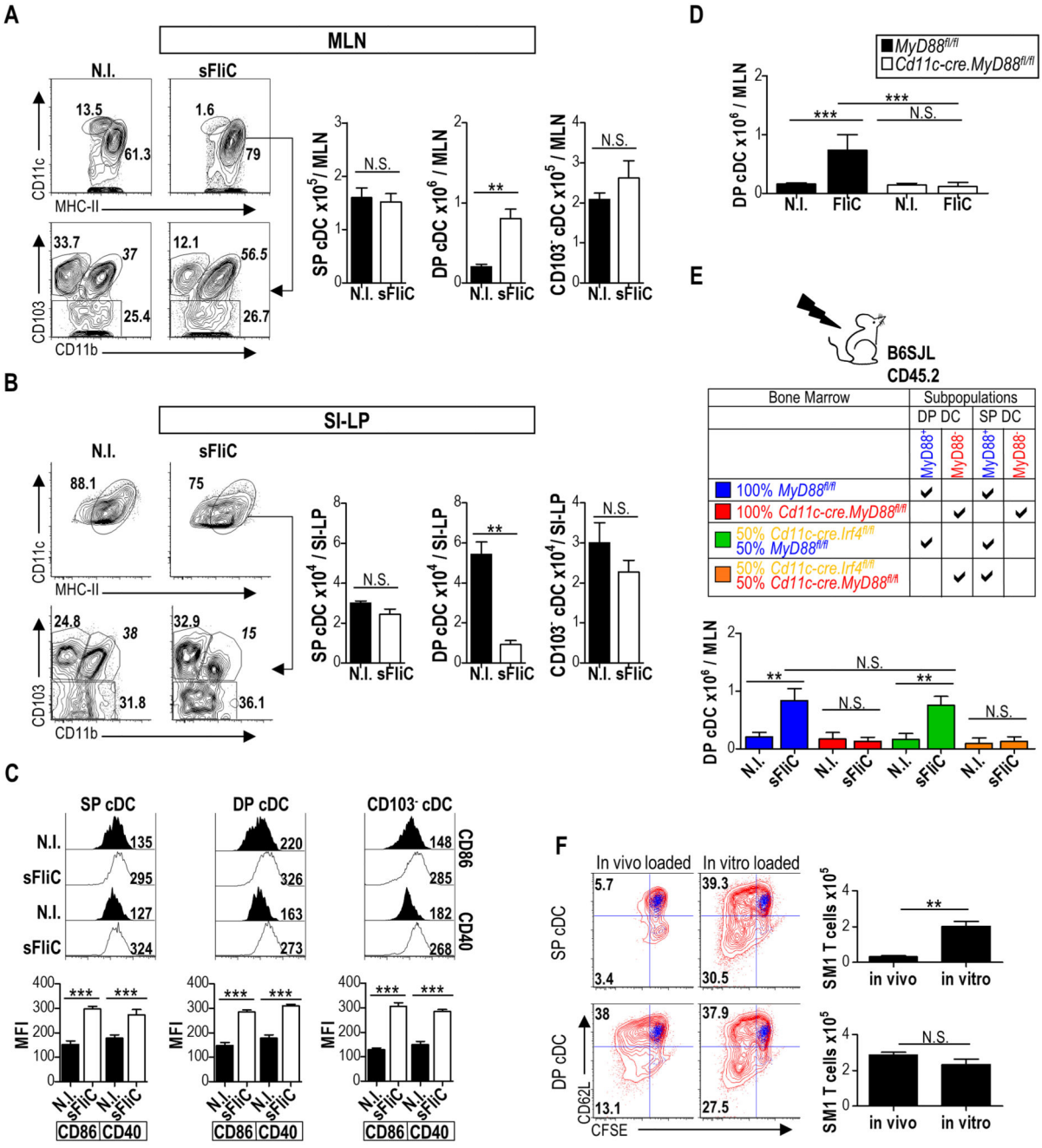


**Figure 1. sFliC stimulates DP cDC directly to induce their accumulation in the MLN and loss from the SI-LP.**

WT mice were immunized i.p with sFliC and cDC (MHC-II$^{+}$CD11c$^{hi}$) subsets evaluated in (a) MLN and (b) SI-LP 24 h later by flow cytometry. Representative plots with percentages for SP, DP and CD103$^{-}$ cDC subsets are shown. Graphs show absolute numbers of the gates. (c) Representative histograms of expression of CD86 and CD40 on SP, DP and CD103$^{-}$ cDC subsets 24 h post sFliC immunization. Graphs show mean fluorescent index (MFI). Data are mean +SD of 4 mice and are representative of 3 independent experiments. ***$p < 0.0001$, by Mann Whitney test. (d) Absolute numbers of DP cDC in the MLN of *Cd11c*-

*cre.MyD88*$^{fl/fl}$(white) or *MyD88*$^{fl/fl}$ (black) mice 24h post sFliC-immunization. Mean +SD (n=6 mice/group) of 2 independent experiments. ***$p < 0.0001$, by two-way ANOVA. (e) Lethally irradiated WT mice were reconstituted with *MyD88*$^{fl/fl}$ or *Cd11c-cre.MyD88*$^{fl/fl}$ BM or with a 50:50 mixture of *MyD88*$^{fl/fl}$ or *Cd11c-cre.MyD88*$^{fl/fl}$ with *Cd11c-cre.Irf4*$^{fl/fl}$ BM. Absolute numbers of DP cDC in the MLN 24h post immunization. Mean +SD (n=8 mice/group) from 2 independent experiments. ***$p < 0.0001$, by two-way ANOVA. (f) MLN SP and DP cDC subsets were FACS sorted from WT mice 24 h post sFliC-immunization and cultured for 4 d with CFSE-labelled FliC-specific transgenic (SM1) T cells in a 1:30 ratio. sFliC (2mg) was added to some cultures (*in vitro* loaded) as indicated. T cell division was assessed by CFSE dilution and CD62L downregulation, blue overlay represents T cells cultured alone, representative plots are shown. Graphs depict absolute numbers of T cells. Data are mean +SD (n=4 mice/group) from two pooled experiments. **$p < 0.001$, by Mann Whitney test.

Europe PMC Funders Author Manuscripts

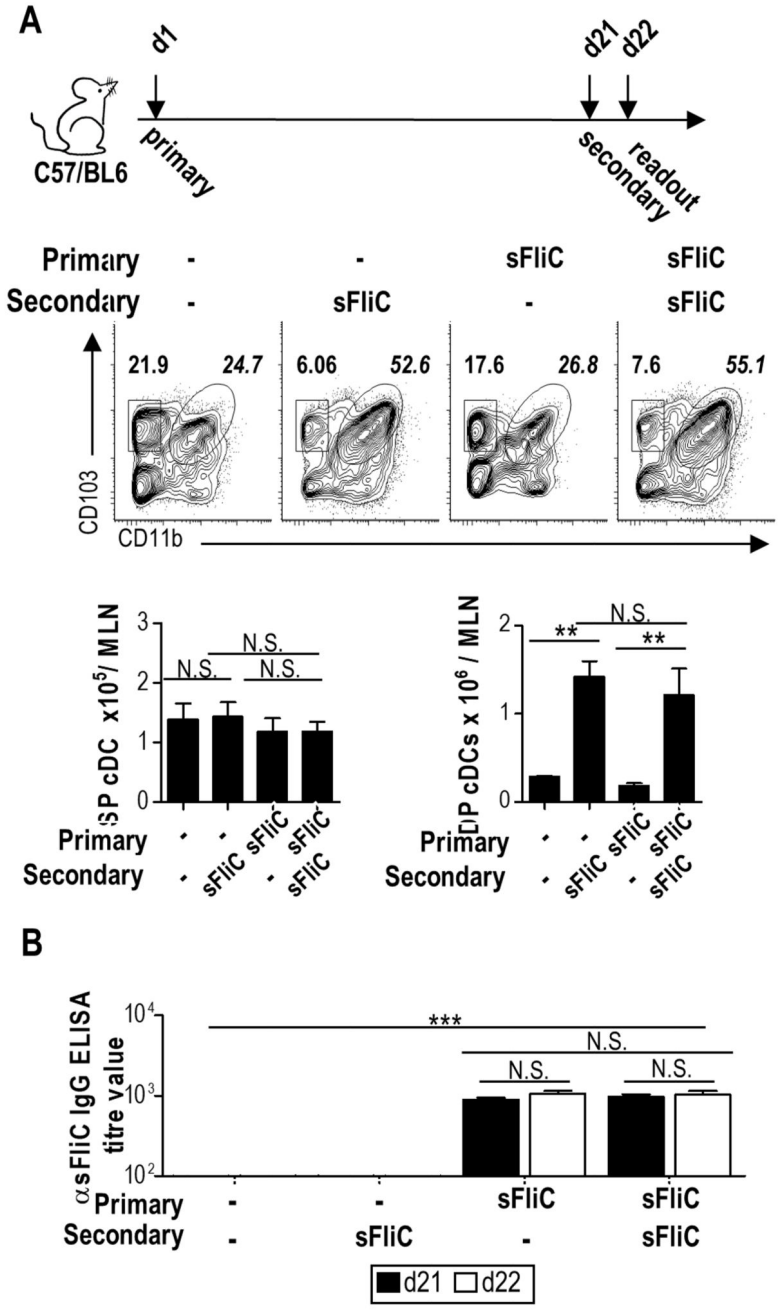


**Figure 2. Secondary sFliC immunization does not affect the MLN cDC accumulation.**

(a) DP and SP cDC accumulation in the MLN of WT mice 24 h after sFliC primary or boost immunization. Representative plots with percentages for SP and DP cDC subsets. Graphs show absolute numbers of the gates. (b) Serum levels of anti-sFliC 21 d post SFliC immunization (black) or 1 d post boost (d22) (white) as indicated. Data are mean +SD (n=4 mice/group) of two independent experiments. $^{**}p < 0.001$, by one way ANOVA.

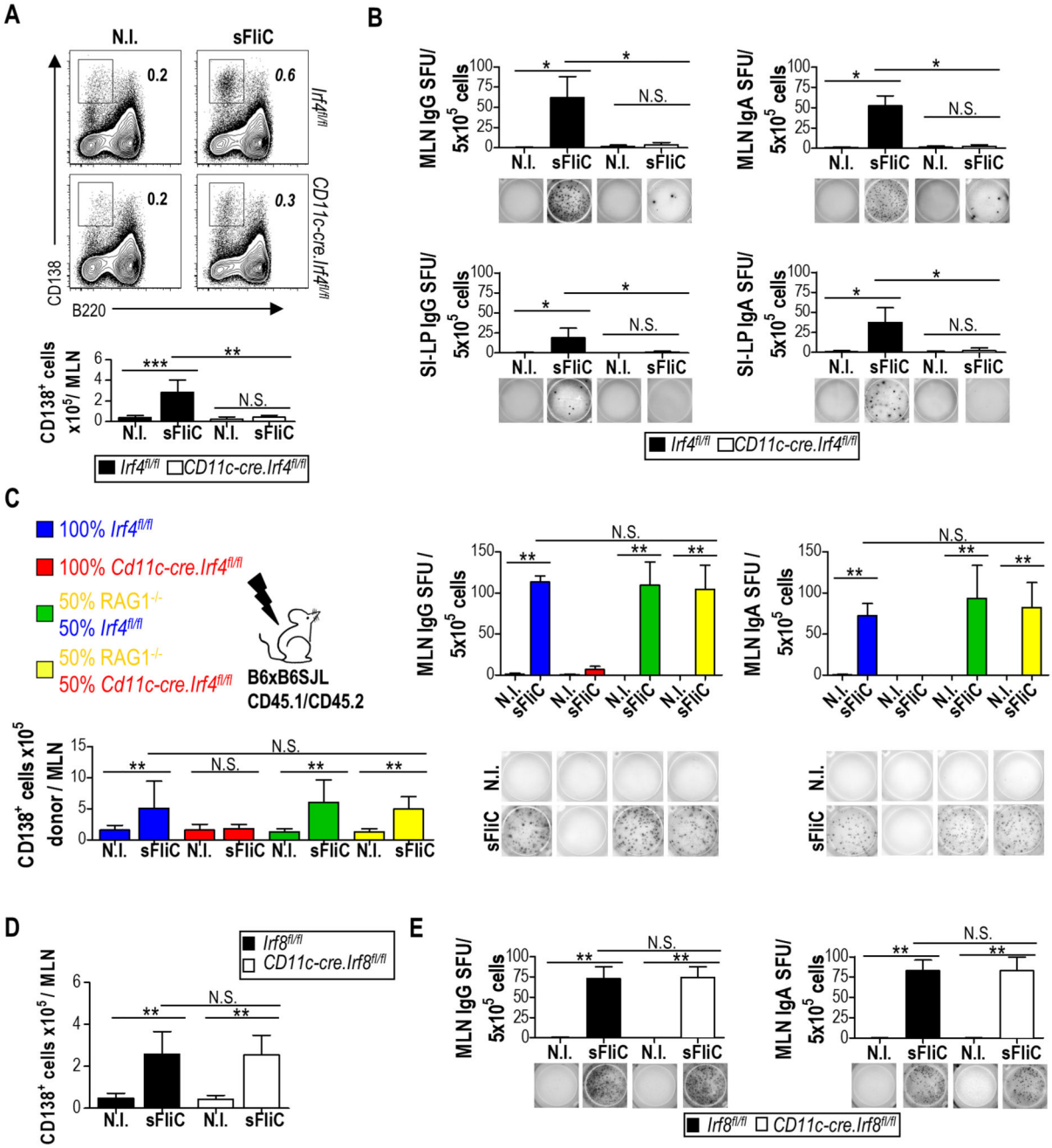


**Figure 3. DP cDC control the induction of the mucosal Ab response to sFliC.**

*Irf4*$^{fl/fl}$ (black) or *Cd11c-cre.Irf4*$^{fl/fl}$ (white) mice were either non-immunized (N.I) or primed and boosted with sFliC. The Ab response was evaluated 4 d post-boost. (a) Representative plots and absolute number (graphs) of plasma cells (TCRb$^{-}$ CD19$^{+}$B220$^{low}$CD138$^{+}$) in the MLN. (b) ELISPOT analysis of sFliC IgG and IgA responses in the MLN and SI-LP. Number of spot-forming units (SFU) per 5x10$^{5}$ cells (graphs) and representative pictures of wells (lower panels). Data are mean +SD (n=4 mice/group) and are from 1 representative experiment of three performed. ***$p < 0.0001$, by two-way

ANOVA. (c) Indicated BM chimeras were either non-immunized (N.I) or sFliC-primed boosted. Total number of $CD45.2^+$ plasma ($CD138^+$) cells (lower left graph), sFliC specific ASC (right upper graphs) and representative ELISPOT wells (lower right) from the MLN of chimeric mice 4 d post-boost. Data are mean +SD (n=4 mice/group). ***$p < 0.0001$, by one way ANOVA. (d and e) *Cd11c-cre.Irf8*$^{fl/fl}$ (white) or *Irf8*$^{fl/fl}$ control mice (black) were either non-immunized (N.I) or sFliC-primed boosted, and the absolute number of (d) plasma cells and (e) sFLiC-specific IgG and IgA ASC in the MLN assessed 4 d post boost. Data are mean +SD (n=8 mice/group) from 2 pooled experiments. ***$p < 0.0001$, by two way ANOVA.



Europe PMC Funders Author Manuscripts

Europe PMC Funders Author Manuscripts

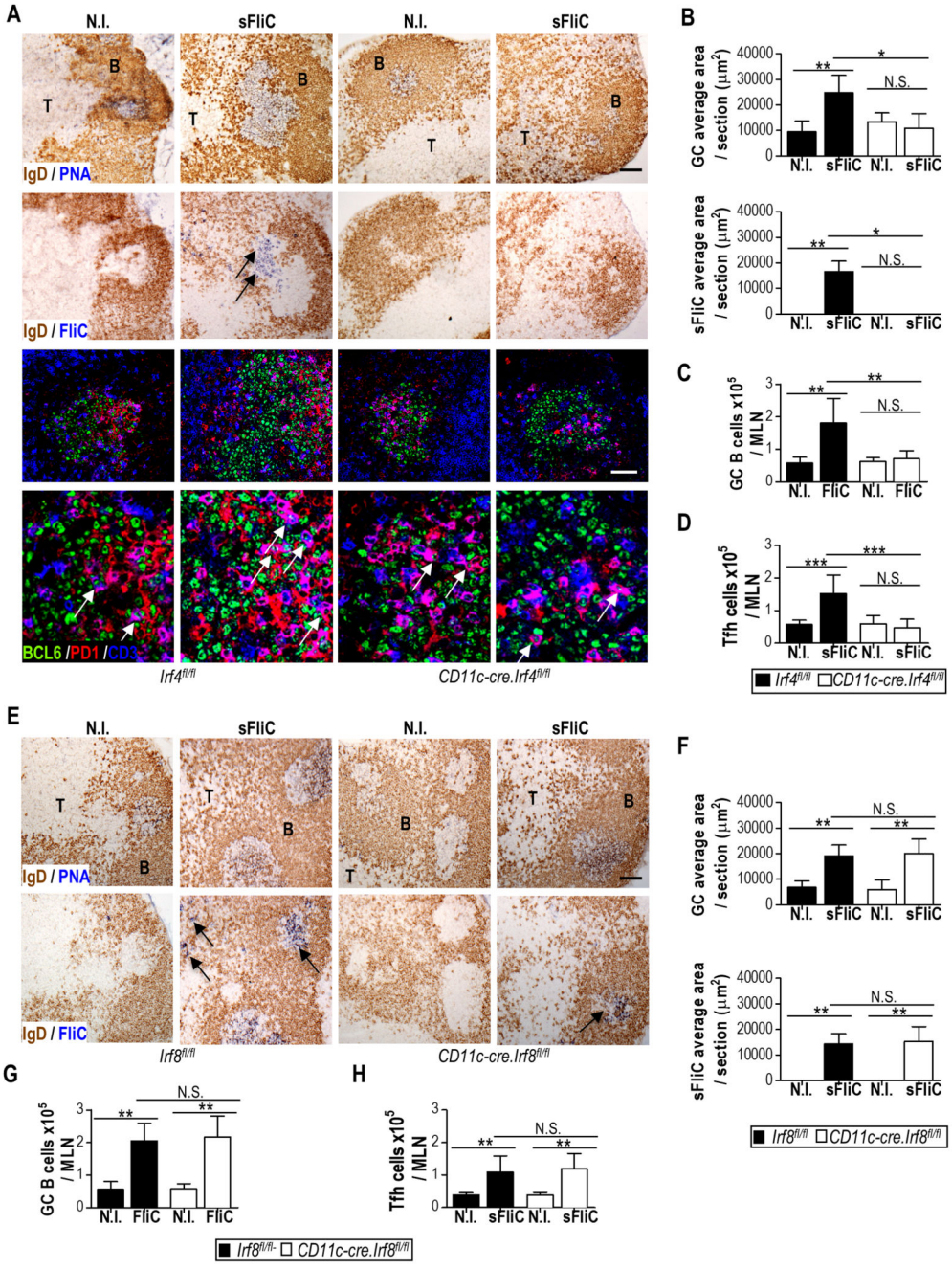


**Figure 4. sFliC-specific GC and Tfh cell induction in the MLN are dependent on DP mucosal cDC.**

(a) Representative photomicrographs of sFliC-specific GC in the MLN of *Irf4*$^{fl/fl}$ (black) or *Cd11c-cre.Irf4*$^{fl/fl}$ (white) non-immunized (N.I) or sFliC prime-boosted mice. Scale bar, 200 mm. First row, GC identification (PNA, blue; IgD, brown). Second row, sFliC-specific GC (sFliC, blue; IgD, brown). Lower panel, confocal analysis of the previously selected GC stained to identify Tfh cells (BCL6, green; PD1, red and CD3, blue). Scale bar, 50 µm. (b) Quantification of total GC and sFliC-specific area per section. Mean +SD (n=10 sections/ group, from 2 experiments). Number of (c) GC B cells (TCR$^{-}$CD138$^{-}$GL7$^{+}$CD95$^{+}$) and (d)

Tfh cells ($CXCR5^+PD1^+$). Mean +SD (n=12 mice/group) from 3 pooled experiments. ***$p < 0.0001$, by two way ANOVA. (e) Representative photomicrographs and (f) quantitation of total GC area and SFliC specific area in serial MLN sections from non-immunized (N.I) or sFliC prime-boosted *Irf8*$^{fl/fl}$ (black) or *Cd11c-cre.Irf8*$^{fl/fl}$ (white) mice. (e) Scale, 200 μm. First row, GC identification (PNA, blue; IgD, brown). Second row, sFliC-specific GC (sFliC, blue; IgD, brown). (f) Mean +SD (n=8 sections/group, from 2 experiments). Number of (g) GC B cells ($TCR^-CD138^-GL7^+CD95^+$) and (h) Tfh cells ($CXCR5^+PD1^+$) as assessed by FACS. Mean +SD (n=8 mice/group) from 2 experiments. **$p < 0.001$, by two way ANOVA.



Europe PMC Funders Author Manuscripts

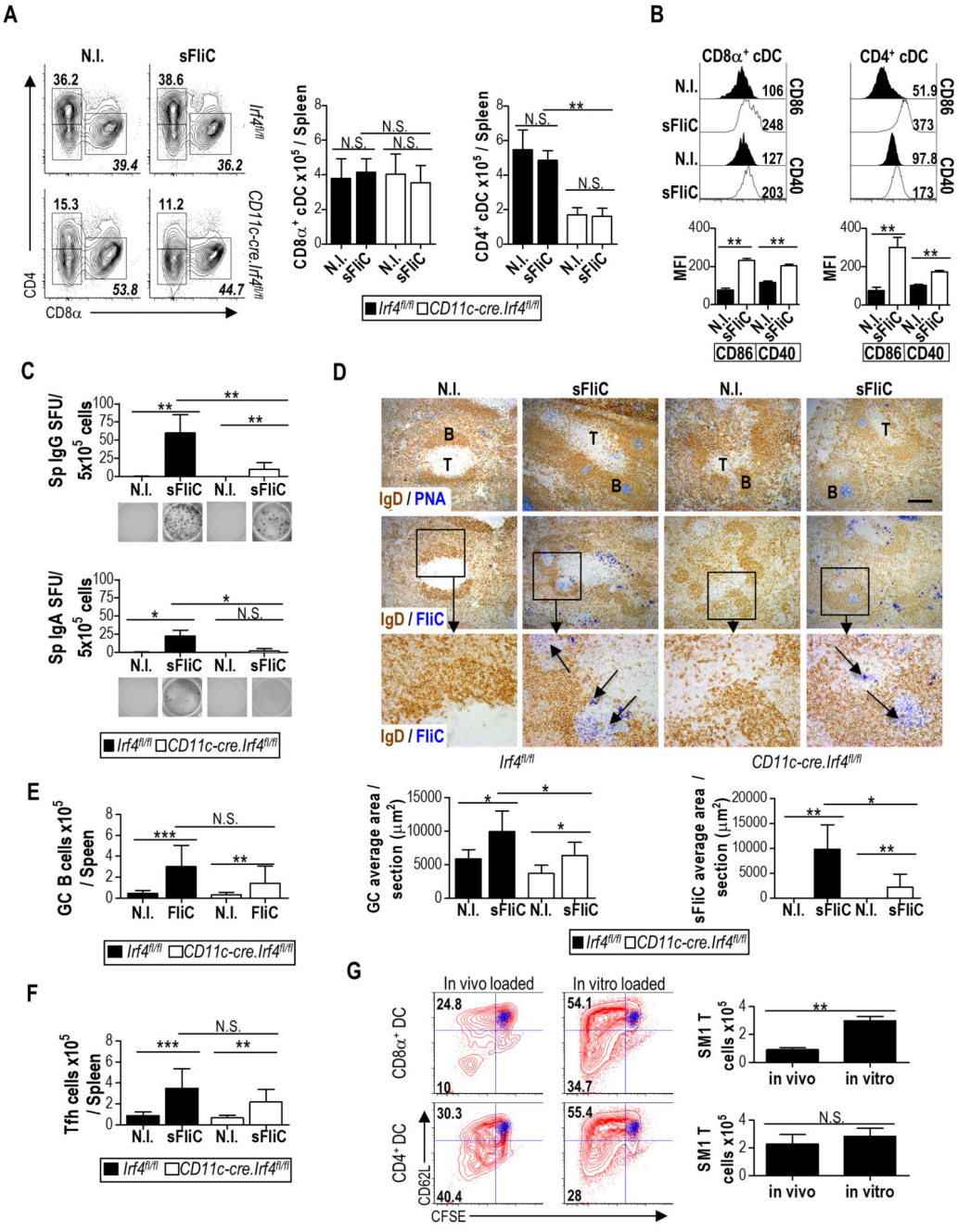


**Figure 5. Systemic responses to sFliC are reduced in the absence of splenic CD4$^+$CD11b$^+$ cDC.**

*Irf4$^{fl/fl}$* (black) or *Cd11c-cre.Irf4$^{fl/fl}$* (white) mice were either non-immunized (N.I) or sFliC prime-boosted. (a) Representative plots (with percentage) and absolute number (right graphs) of CD4$^+$ and CD8α$^+$ splenic cDC. (b) Representative histograms and pooled mean fluorescence intensity (MFI) of CD86 and CD40 levels on CD4$^+$ and CD8α$^+$ splenic cDC subsets 24 h post sFliC immunization. Mean +SD (n=4 mice/group) from 1 representative experiment of 3 performed. ***$p < 0.0001$, by two-way ANOVA. (c) ELISPOT analysis of splenic sFliC-specific IgG and IgA cells. Lower panels show representative pictures. Mean

+SD (n=12 mice/group) of 3 experiments. $^{**}p < 0.001$, by two way ANOVA. (d) Representative micrographs of (first row) GC (PNA, blue; IgD, brown), (second row), sFliC-specific GC (sFliC, blue; IgD, brown) and (last row), high magnification of identified area. Scale bar represents 200 μm. Quantification of total GC area and sFliC-specific area per section. Mean +SD (n=10 sections/group), of 2 experiments. Total number of (e) Splenic GC and (f) Tfh cells ($CXCR5^+PD1^+$) cells. Mean +SD (n=12 mice/group) of 3 experiments. $^{***}p < 0.0001$, by two way ANOVA. (g) $CD4^+$ and $CD8\alpha^+$ splenic cDC subsets were cell sorted (97% purity) from WT mice 24h after immunization with sFliC and cultured for 4 d with CFSE-labeled SM1 transgenic T cells in a 1:30 ratio. cDC were used a sorted (*in vivo* loaded) or additional 2mg of sFliC was added to the culture (*in vitro* loaded). T cell division was assessed by CFSE dilution and CD62L expression, blue overlay represents culture of only T cells. Representative histograms from three independent experiments are shown. Data are shown as mean +SD (n=4 mice/group) and are representative of two independent experiments polled together. $^{**}p < 0.001$, by Mann Whitney test.



Europe PMC Funders Author Manuscripts

Europe PMC Funders Author Manuscripts

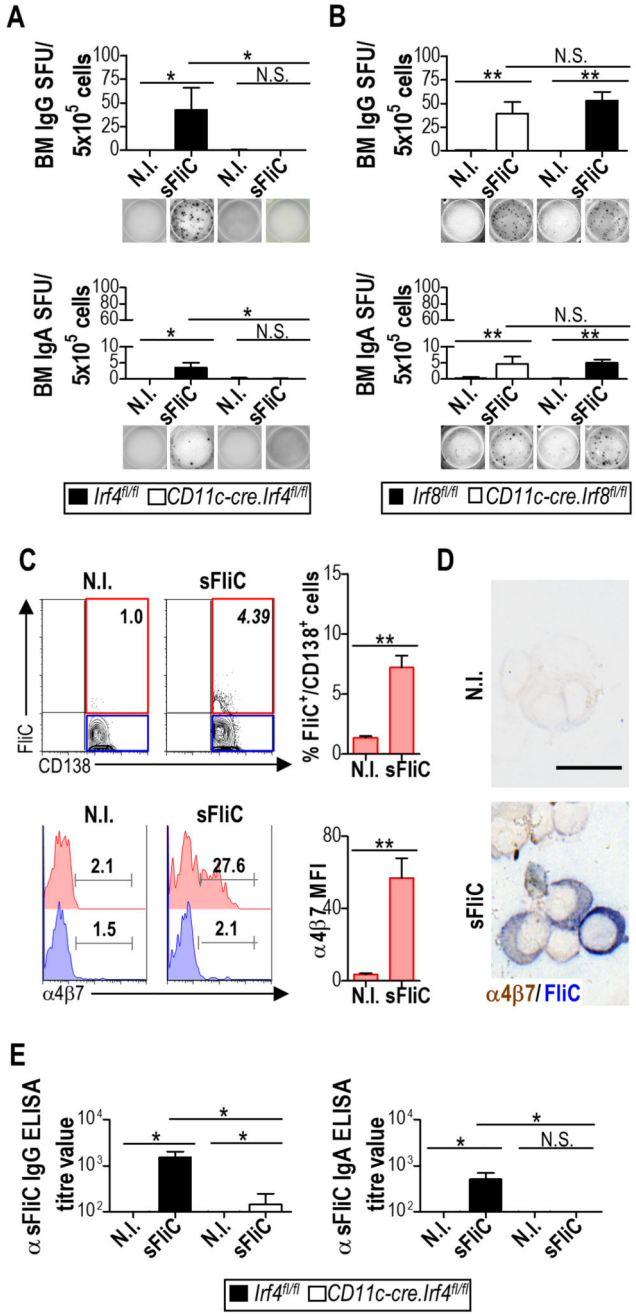


**Figure 6. The mucosal response to sFliC contributes to the systemic antibody response.**

*Irf4*$^{fl/fl}$ (black) or *Cd11c-cre.Irf4*$^{fl/fl}$ (white) mice were either non-immunized or sFliC prime-boosted. (a) ELISPOT analysis of sFliC IgG and IgA responses in the BM. Number of spot-forming units (SFU) per 5x10$^5$ cells (graphs) and representative pictures of wells (lower panels). Data are shown as mean +SD (n=12 mice/group) of three independent experiments pooled together. ***$p < 0.0001$, by two-way ANOVA. (b) *Cd11c-cre.Irf8*$^{fl/fl}$ (white) or *Irf8*$^{fl/fl}$ control mice (black) were either non-immunized or sFliC-primed boosted. ELISPOT analysis of sFliC IgG and IgA responses in the BM. Data are shown as mean +SD

(n=8 mice/group) of two independent experiments pooled together. *$p < 0.01$, by two way ANOVA. (c) WT mice were non-immunized or sFliC primed-boosted. BM $CD138^+$ cells were intracellularly stained with sFliC-biotynilated, expression of α4β7 is shown in $sFliC^+$ and $sFliC^-$ $CD138^+$ cells by FACS and (d) cytospins show α4β7 (brown) and sFliC (blue) in pre-enriched $CD138^+$ cells. Scale bar indicates 20 μm. Representative plots and photomicrographs (n=4 mice/group) from 2 independent experiments. (e) Serum anti-sFliC IgG and IgA evaluated by ELISA. Data are shown as mean +SD (n=12 mice/group) and are representative of three independent experiments pooled together. ***$p \leq 0.0001$, by two way ANOVA.



Europe PMC Funders Author Manuscripts